Bull. Mater. Sci., Vol. 26, No. 7, December 2003, pp. 749–754. © Indian Academy of Sciences.

Influence of fretting on the fatigue strength at the vise clamp–specimen interface

ABDULHAQQ A HAMID* and RAFI K YAHYA

Mechanical Engineering Department, College of Engineering, University of Mosul, Mosul, Iraq
*Presently at the Mechanical and Industrial Engineering Department, Indian Institute of Technology, Roorkee 247 667, India

MS received 20 April 2002; revised 18 September 2003

Abstract. Fretting fatigue is one of the most important phenomena for inducing a significant reduction of fatigue strength and consequently, leading to unexpected failure accidents of the engineering structures even at very low stresses. In the present study, both plain and fretting fatigue tests with zero mean stress were carried out on two different types of steel, low-carbon steel and martensitic stainless steel, by means of a reversed bending fatigue testing machine. The drop in the fatigue strengths through fretting at vise clamp–specimen interface were significant for both tested steels. The fretting processes produced a reduction in fatigue strength of about 27% for low-carbon steel and 16% for martensitic stainless steel.

Keywords. Plain fatigue; fretting fatigue; low-carbon steel; stainless steel.

1. Introduction

The fatigue strength of a component can be significantly reduced by a process known as 'fretting'. Fretting fatigue occurs at the contact surface between pairs of closely contacting machine components which are not intended to move relative to each other due to component deflections, where the relative microslip (approximately ranging from a few to 250 μm (Neal and Gee 2001), 0 to 50 μm (Waterhouse 1972)) at the interface between two surfaces in intimate contact plays an important role. Many practical examples of fretting fatigue failure are available (Fuchs and Stephens 1980). The most important examples of premature failure from fretting fatigue are those of railway axles onto which the wheel was press-fitted or shrunk and the joint between an aircraft propeller and its hub. Other examples are screws or bolts and nuts, keyed joints, couplings, joints between wire or wire rope etc.

A number of factors influence fretting fatigue behaviour. It has been reported by Dobromirski (1992) that there are more than fifty factors that influence the fretting fatigue behaviour, including the contact pressure, amplitude of relative slip, mean stress, contact materials, surface condition, frequencies of alternating stress and slip etc. Significant efforts by researchers have lead to general understanding of the influences of these factors on fretting fatigue behaviour (Nishioka and Hirakawa 1969; Nakazawa *et al* 1992; Satoh 1992; Waterhouse 1992; Lindley 1997; Gnanamoorthy and Rosi Reddy 2002, etc). Fretting process was found to reduce the fatigue strength in all the investigations but the degree of strength reduction widely varied due to many influencing parameters and the test methodology followed.

The objective of the present work was to investigate the fretting fatigue process that occurs at the vise clamp–specimen interface by utilizing two different shapes of test specimens. Preliminary investigations carried out on the fretting fatigue behaviour of as-received low-carbon steel and martensitic stainless steel are reported. Relative slip, crack initiation, direction and failure are also studied.

2. Experimental

2.1 *Test materials*

Both plain and fretting fatigue tests were conducted on two types of steel: (i) low carbon steel and (ii) martensitic stainless steel. Both cold rolled sheets of 1 mm thickness, with chemical compositions are given in table 1. The static mechanical properties under normalized conditions were determined from standardized specimens using a universal tensile testing machine. Results of the tensile strength and hardness are given in table 2.

Figure 1 shows the configuration and dimensions of plain fatigue and fretting fatigue specimens. The plain fatigue specimen was designed so that the failure occurred outside the vise clamp–specimen interface and the fretting fatigue specimen was designed to produce the failure at

*Author for correspondence

Table 1. Chemical composition of the specimens.

Material	%C	%Si	%Mn	%P	%S	%Cr	%Mo	%Fe
Low-carbon steel	0·17	0·05	0·29	0·05	–	–	–	Rem.
Martensitic stainless-steel	0·1–0·15	1·0	1·5	0·06	0·15–0·35	15·5	0·2	Rem.

Table 2. Static mechanical properties of the specimens.

Material	E (GPa)	S_y (MPa)	S_u (MPa)	% Elong.	HRB
Low-carbon steel	206	199	384	29	36
Martensitic stainless-steel	186	397	648	38·6	76

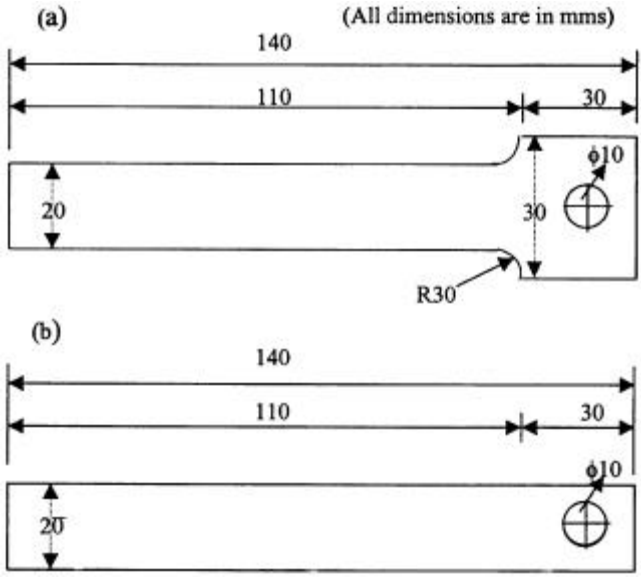

Figure 1. Dimensions and shapes of the specimens: (a) plain fatigue specimen and (b) fretting fatigue specimen.

the vise clamp–specimen interface at the same alternating stress levels. The electrical resistance strain gauges technique was used for determining the alternating stress distribution within the specimen. The clamping device used in fatigue testing machine for gripping the tested specimen was made from two pieces of medium-carbon steel, each of which had a dimension of 60 mm length, 30 mm width and 10 mm thickness, whose chemical composition and mechanical properties are shown in tables 3 and 4, respectively.

2.2 *Fretting fatigue testing machine*

Fatigue and fretting fatigue tests were carried out using a reversed bending testing machine, designed and constructed by us (Abdulhaqq 1997) under a load controlled condition of $R = -1$ at a frequency of 4 Hz. Figure 2a shows a schematic view of the reversed bending testing machine used in the current investigation and figure 2b the photographic view of this machine. The clamping pressure was determined by strain gauges attached directly to the clamping device. The tests were carried out under a controlled and constant pressure of 8·5 MPa. The relative microslip between vise clamp and specimen was measured using a specially designed transducer. Finally all tests were carried out in laboratory air and no special considerations were given to temperature and humidity.

Table 3. Chemical composition of the clamping device material.

%C	%Si	%Mn	%P	%S	%Fe
0·31	0·22	0·55	0·023	0·04	Rem.

Table 4. Static mechanical properties of the clamping device material.

E (GPa)	S_y (MPa)	S_u (MPa)	% Elong.	HRC
209	296	580	34	31

3. Results and discussion

3.1 *Observation of fretted surface*

The appearance of wear debris usually gives us good clue as to where fretting process is suspected. Figure 3 is a magnified photograph of the damaged surface which was observed after 10^5 cycles of fretting, where the alternating stress and the amplitude of fretting slip are 183 MPa and 27 μm, respectively. After a few hundred of cycles, visible fretting corrosion begins to appear near the vise clamp–specimen interface. The generated wear debris is much redder than the normal rust observed on

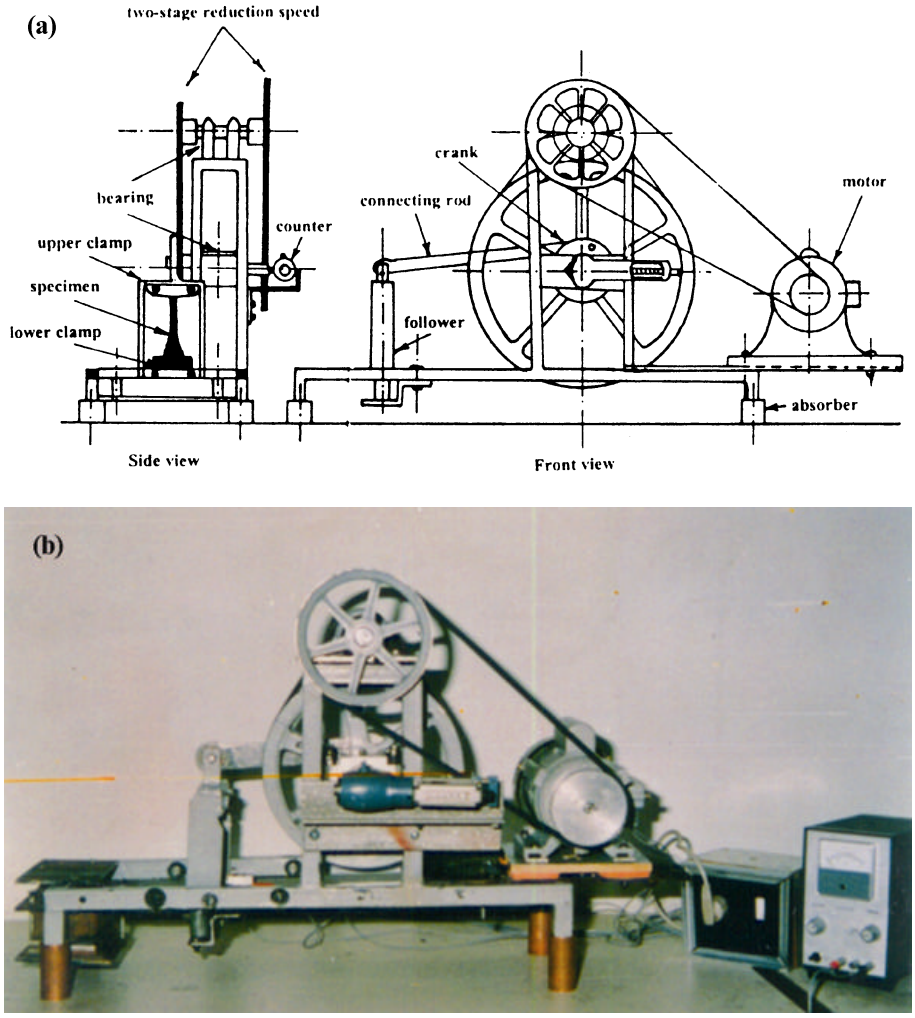

Figure 2. (**a**) A schematic view of the reversed bending testing machine and (b) photographic view of this machine.

the surface damage, these wear debris plays an important role in accelerating the crack initiation process in the damaged surface.

Microscopic examination of the fretted surface shows a large number of cracks as shown in figure 4. Some types of cracks leading to the final fracture of the fretting specimens were reported (Endo and Goto 1976; Lamacq *et al* 1992; Gnanamoorthy and Rosi Reddy 2002). Cracks were initiated on a plane inclined about 35° to the surface in a very early stage of fatigue life. The cracks then changed their direction of propagation to approximately normal to the surface. Cracks emanating from the fretting zone grow perpendicular to the fretting zone without clear stage I and II types. In this study, most of the cracks showed clear stage I and II types of cracks growth. The cracks initiated at the edge of the fretting area in all the specimens. The stage I crack angle ranging from 21–43° were observed for all the tested specimens.

3.2 *Relative slip*

When a specimen is subject to a cyclic bending loading, a minute cyclic relative slip was observed between the specimen near the end and the upper edge of the vise clamp due to the repeating elongation and contraction of the specimen fibres. The slip takes place in the opposite direction on each side of bending axis.

A special kind of transducer was made with compact size and performance of high sensitivity for measuring the relative slip. An example of the results obtained for the variation of the relative slip at the vise clamp–specimen interface with the number of cycles (for low-carbon specimen and at alternative stress of 85 MPa) is shown in figure 5 (which is recorded after an average of 5×10^3 cycles). The relations between the relative slip amplitude at the vise clamp–specimen interface and the alternating bending stress at the end of specimen and for both tested steels are shown in figure 6. It is shown from

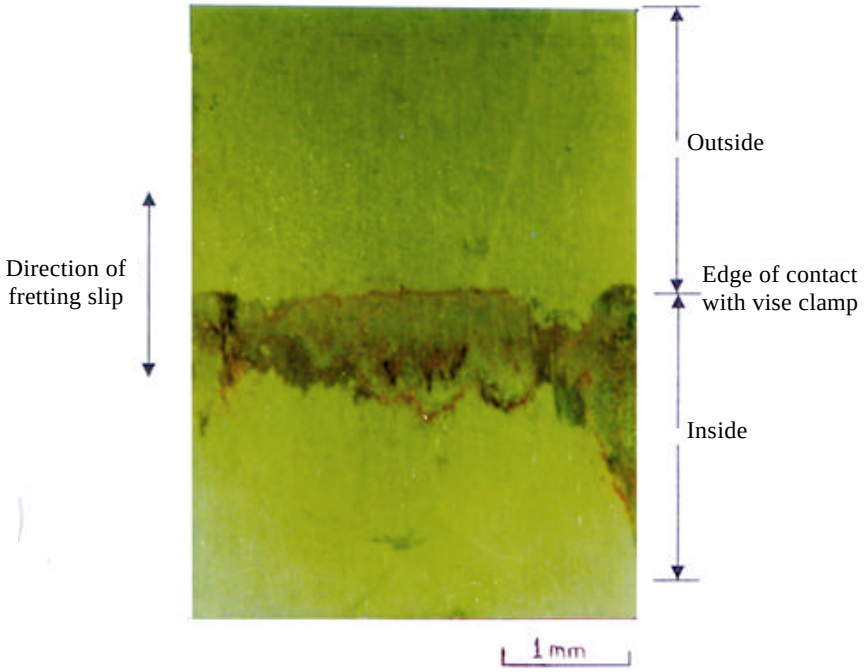

Figure 3. Macroscopic appearance of fretted area for carbon steel specimen.

the figure that for smaller alternating stresses (< 140 MPa for low-carbon steel and < 220 MPa for martensitic stainless steel), the correlation exhibits linearity, while for larger alternating stresses (greater than the above values), the relative slip increases rapidly with the increase of the alternating stresses. The possible reason for this rapid increase is attributed to the plastic deformation of the outer specimen fibres due to large alternating stress.

3.3 *Plain and fretting fatigue*

The S–N diagrams for plain and fretting fatigue tests are shown in figures 7–10 for both the tested steels. The experimental plain and fretting fatigue limits were defined as the runout stress amplitude at 5×10^6 cycles. The resulting fatigue limits for both tests in these materials are listed in table 5. The ratio between the plain bending fatigue limit and tensile strength were found as 0·51 for low-carbon steel and 0·48 for martensitic stainless steel. In general, the plain fatigue limits are half of the tensile strengths in these materials.

The general linear relationship between S_a and N_f for constant amplitude loading can be given as

$$N_f \cdot S_a^m = c. \quad (1)$$

The values of m and c obtained in the present study are listed in table 6. In the case of fretting, as the number of reversal cycles of fretting increases the wear grows gradually on both mating surfaces and the iron oxide particles

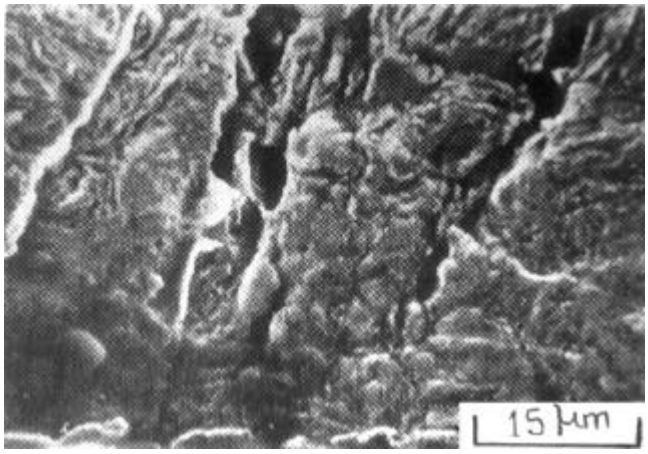

Figure 4. Crack initiation region in fretting fatigue (S_a = 183 MPa).

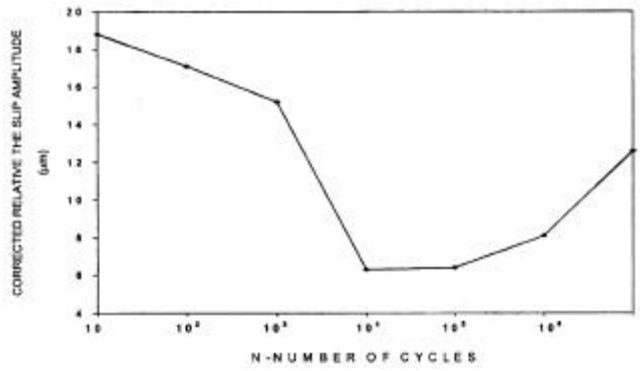

Figure 5. Variation of relative slip amplitude at the vise clamp–specimen interface with the number of cycles.

(debris) are observed to flow out from the fretted regions. So, the fatigue reduction strength is of the lowest value in the short-life region, then the reduction gradually increases as the number of cycles increases.

From the S–N diagrams of each tested steel and from table 6, we can easily observe that the slope of fretting curve increased due to fretting action, i.e. the fatigue life under fretting action is shorter than those under normal fatigue test. Above the knee of the S–N diagram, the damage occurred from the combination of fatigue and fretting actions, while below the knee the damage is solely due to fretting action.

In the case of low-carbon steel, the specimen is fretted with the vise clamp for about 5×10^6 cycles under a constant pressure and the amplitude of slip of about 18 μm. The fretting process produced a reduction in the fatigue limit from 191 MPa to 138 MPa. Similar comparison were applied for the martensitic stainless, the fretting process produced a reduction in the fatigue limit from 316·5 MPa to 265 MPa. It is apparent that the fatigue limits of the tested steels are significantly reduced by fretting actions. Therefore, the low-carbon steel suffers the greatest relative reduction in the fatigue limit due to fretting action.

There are two important factors which may considerably affect these results. Firstly, the difference of the surface roughness between the tested steels. The measured surface roughness for both tested steels are R_a = 1·26 μm for low-carbon steel specimen and R_a = 0·35 μm for martensitic stainless steel specimen. According to Waterhouse (1972), with the higher degree of surface finish the more serious is fretting damage. Secondly, the compressive-residual stresses in tested steel sheets are due to cold rolling process. Mutoh (1988) found that the compressive-residual stresses were the most favourable and

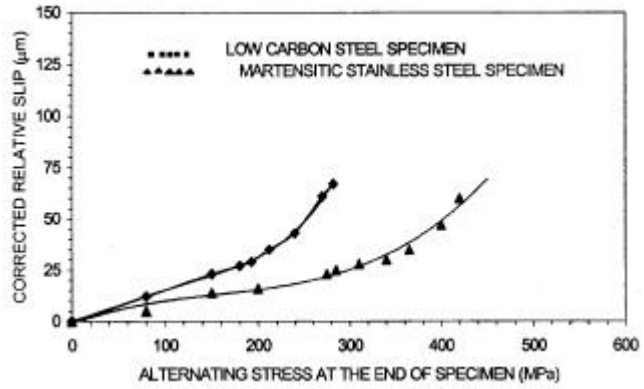

Figure 6. Variation of the slip amplitude with the alternating stress for both tested steels.

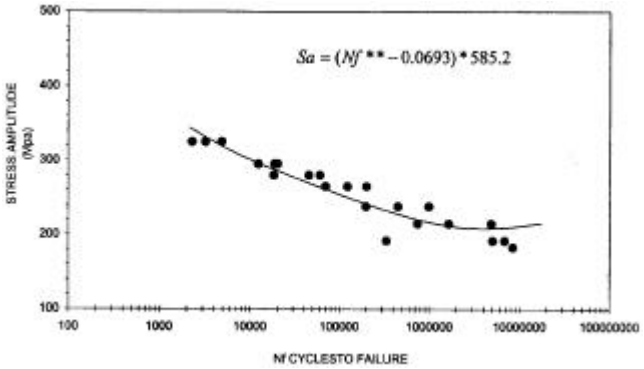

Figure 7. S–N diagram for plain fatigue of the low-carbon steel.

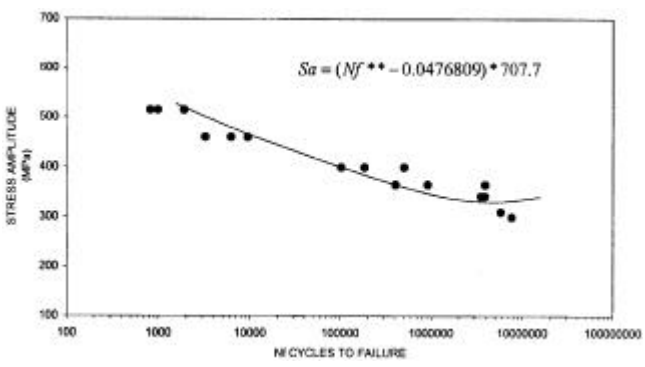

Figure 8. S–N diagram for plain fatigue of the martensitic stainless steel.

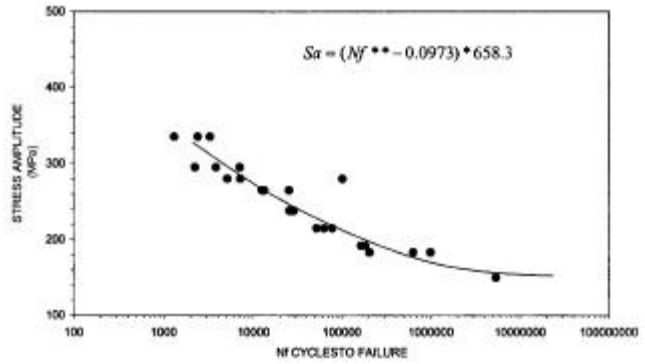

Figure 9. S–N diagram for fretting fatigue of the low-carbon steel.

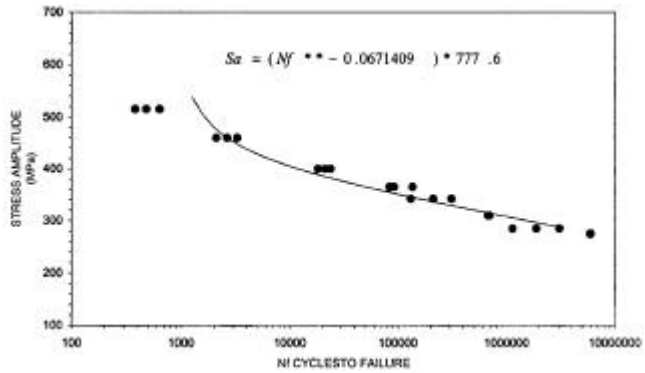

Figure 10. S–N diagram for fretting fatigue of the martensitic stainless steel.

Table 5. Plain and fretting fatigue limits and strength reduction factors of the tested steels.

Material	S_{pf} (MPa)	S_{pf}/S_u	S_{ff} (MPa)	SRF
Low-carbon steel	191	0·51	138	1·39
Martensitic stainless-steel	316·5	0·48	265	1·19

Table 6. Characterized constants for the S–N diagrams of tested steels.

	Low-carbon steel		Martensitic stainless-steel	
Test method	m	C	m	C
Plain fatigue	14·50	$1{\cdot}33 \times 10^{40}$	20·83	$2{\cdot}35 \times 10^{59}$
Fretting fatigue	10·31	$1{\cdot}14 \times 10^{29}$	14·93	$1{\cdot}40 \times 10^{43}$

improves the fatigue and fretting fatigue strengths of the materials.

4. Conclusions

The plain and fretting fatigue tests with zero mean stress ($R = -1$) were carried out using two different types of steel. The characteristics of fretting fatigue was discussed. The micro relative slip results are obtained and discussed as they vary with the alternating stress. The main results are summarized as follows: the fretting processes produced a reduction in fatigue strength of about 27% for low-carbon steel and 16% for martensitic stainless steel. Hence, the martensitic stainless steel has a high resistance to fretting fatigue compared with the low-carbon steel.

Nomenclature

E,	modulus of elasticity	:	(Pa)
M,	bending moment	:	(N.m)
$M\&C$,	characterize constants of an S–N diagram	:	(–)
N_f,	number of stress cycles to failure	:	(cycle)
P,	applied load	:	(N)
R,	stress ratio, ratio of the minimum to the maximum stress	:	(–)
R_a,	average departure of the surface from perfection over a sampling length (0·8 mm)	:	(μm)
S_a,	alternating stress amplitude	:	(Pa)
S_{ff},	fretting fatigue limit	:	(Pa)
S_{pf},	plain fatigue limit	:	(Pa)
SRF,	strength reduction factor	:	(–)
S_u,	ultimate tensile strength	:	(Pa)
S_y,	yield tensile strength	:	(Pa)

References

Abdulhaqq A Hamid 1997 *Studying the effect of fretting on the fatigue strength of steels*, M.Sc. Thesis, University of Mosul, Iraq

Dobromirski J M 1992 *Standardization of fretting fatigue test methods and equipment, STP 1159* (Philadelphia, USA: ASMS) p. 60

Endo K and Goto H 1976 *Wear* **38** 311

Fuchs H O and Stephens R I 1980 *Metal fatigue in engineering* (New York: John Wiley and Sons, Inc.)

Gnanamoorthy R and Rosi Reddy R 2002 *Bull. Mater. Sci.* **25** 109

Lamacq V *et al* 1992 *Tribology Int.* **30** 391

Lindley T C 1997 *Int. J. Fatigue* **19** 539

Mutoh Y and Tanaka K 1988 *Wear* **125** 175

Nakazawa K *et al* 1992 *Standardization of fretting fatigue test methods and equipment, STP 1159* (Philadelphia, USA: ASMS) p. 115

Neal M J and Gee M 2001 *Wear problems and testing for industry* (Great Britain: William Andvew. Publishing)

Nishioka K and Hirakawa K 1969 *JSME Int. J.* **12** 397

Satoh K 1992 *Standardization of fretting fatigue test methods and equipment, STP 1159* (Philadelphia, USA: ASMS) p. 85

Waterhouse R B 1972 *Fretting corrosion* (Oxford: Pergamon Press)

Waterhouse R B 1992 *Int. J. Fatigue* **37** 77